Anal. Chem. **1997,** *69,* 679−687

Molecular Design of Intercalation-Based Sensors. 1. Ammonia Sensing with Quartz Crystal Microbalances Modified by Copper Biphenylbis(phosphonate) Thin Films

Louis C. Brousseau, III, and Thomas E. Mallouk*

Department of Chemistry, The Pennsylvania State University, University Park, Pennsylvania 16802

By combining the shape-selective intercalation reaction of ammonia into copper biphenylbis(phosphonate) with the nanogram sensitivitiy of the quartz crystal microbalance (QCM), it is possible to detect ammonia at gas-phase concentrations of 0.01−25%. Anhydrous copper biphenylbis(phosphonate), $Cu_2(O_3PC_6H_4-)_2$, precipitates as lamellar microcrystals when solutions of Cu^{2+} and biphenylbis(phosphonic acid) are combined, and its structure is closely related to that of $Cu(O_3PC_6H_5)$. Well-ordered and oriented thin films of this material were assembled on the gold electrodes of QCM devices by sequential adsorption of copper salts and biphenylbis(phosphonic acid). Ammonia intercalation occurs at two sites on the lattice copper atoms, one of which is irreversible at room temperature. Larger Lewis bases, such as butylamine isomers, are substantially excluded from the ammonia binding sites. The transport of ammonia into the films, which was monitored by the frequency change of the QCM device, is characterized by an effective diffusion coefficient of 5.6×10^{-9} cm^2/s. With ultrathin (<70 Å) self-assembled films, the device reponse is relatively rapid and the ammonia intercalation reaction is 90% complete in 90 s or less.

The sensing of gaseous substances has become increasingly important in recent years for applications in environmental, industrial, and biomedical monitoring. The sensing of ammonia is particularly important because of its use as a reagent in the production of fertilizers and other nitrogen-containing compounds. It is a byproduct of many industrial and agricultural activities, such as the breakdown of sewage and garbage, and ammonia therefore appears in wastewater and runoff streams.[1] Because it is a product of biochemical processes, ammonia is also a useful reporter molecule in a variety of applications, for example, as an indicator of the freshness of fish,[2] in the detection of diseases of the liver, and as a probe of protein metabolism.[3]

Although ammonia levels can be determined accurately in some applications through acid−base titration, this process does not lend itself to automated, continuous, or repeated monitoring. For this reason, research on automated, and preferably portable, ammonia sensors has grown markedly in recent years. Ammonia sensors recently described in the literature have taken advantage of optical or electrochemical responses in both liquids and vapors and operate over a broad range of conditions and concentrations. One class of solid-state ammonia sensors relies on a change in the resistivity, which is caused by adsorption of the analyte to the surface of semiconducting metal oxides[4−6] or ionic conductors.[7,8] These devices usually operate at somewhat elevated temperatures (>100 °C) and are also sensitive to combustible gases and water vapor. Optical sensors detect ammonia by the change in absorbance of an acid−base indicator,[1,9−13] the fluorescence of an ammoniacal complex,[14] or a change in refractive properties of a coating.[3,15] This group of sensors operates at room temperature, but is also sensitive to water levels in the cell or in the polymer membrane, and several are irreversible. A sensor based on a bulk acoustic wave (BAW) device incorprates an ion-selective coating that is specific for ammonia.[16] The basis for signal transduction with this device is similar to that of the sensor described in this paper, although the chemical reaction is quite different. Table 1 summarizes the operating characteristics, range of sensitivity, response times, and reversibility of some of these ammonia sensors.

Gas sensors that are based on the intercalation of solid-state materials, such as lamellar chalcogenides, are often very sensitive. Unfortunately, the intercalation process is usually nonspecific, and chemically similar analytes can give substantial interferences. Additionally, the response time and reversibility of these devices is generally poor because of solid-state diffusion effects.[17] Sensors

(1) Andrew, K. N.; Worsfold, P. J.; Comber, M. *Anal. Chim. Acta* **1995**, *314*, 33.
(2) Maekawa, T.; Tamaki, J.; Miura, N.; Yamazoe, N. *Chem. Lett.* **1992**, 639 and references therein.
(3) Smock, P. L; Orofino, T. A.; Wooten, G. W.; Spencer, W. S. *Anal. Chem.* **1979**, *51*, 505.
(4) Shaver, P. J. *Appl. Phys. Lett.* **1967**, *11*, 255.
(5) Rosse, G.; Ghers, M.; Lebigot, J.; Guyader, J. Laurent, Y.; Colin, Y. *Sens. Actuators* **1988**, *14*, 133.
(6) Moseley, P. T.; Williams, D. E. *Sens. Actuators, B* **1990**, *40*, 113.
(7) Lauer, U.; Maier, J.; Göpel, W. *Sens. Actuators, B* **1990**, *40*, 125.
(8) Mayo, N.; Harth, R.; Mor, U.; Marouani, D.; Hayon, J.; Bettelheim, A. *Anal. Chim. Acta* **1995**, *310*, 139 and references therein.
(9) Arnold, M. A.; Ostler, T. J. *Anal. Chem.* **1986**, *58*, 1137.
(10) Çağlar, P.; Narayanaswamy, R. *Analyst* **1987**, *112*, 1285.
(11) Liu, S.; Dasgupta, P. K. *Anal. Chim. Acta* **1995**, *308*, 281.
(12) Wolfbeis, O. S.; Posch, H. E. *Anal. Chim. Acta* **1986**, *185*, 321.
(13) Ozawa, S.; Hauser, P. C.; Seiler, K.; Tan, S. S. S.; Morf, W. E.; Simon, W. *Anal Chem.* **1991**, *63*, 640.
(14) Genfa, Z.; Dasgupta, P. K. *Anal. Chem.* **1989**, *61*, 408.
(15) Giuliani, J. F.; Wohltjen, H.; Jarvis, N. L. *Opt. Lett.* **1983**, *8*, 54.
(16) Xu, Y.; Si, S.; Lu, C.; Nie, L.; Yao, S. *Anal. Chim. Acta* **1995**, *312*, 9.
(17) (a) Whittingham, M. S., Jacobson, A. J., Eds. *Intercalation Chemistry;* Academic Press: New York, 1982; (b) Atwood, J. L., Davies, J. E. D., MacNicol, D. D., Eds. *Inclusion Compounds;* Academic Press: London, 1984.

S0003-2700(96)00630-0 CCC: $14.00

Table 1. Properties of Some Optical and Electrochemical Ammonia Sensors

sensing method	detection range	conditions	response time	ref
waveguide	0−40 ppm	ambient, air	30 min, irrev	3
waveguide	60−1000 ppm	ambient, air	3 min, rev	15
abs/fluor	1−100 ppm	ambient, air	28 min, rev	1
abs/fluor	4−340 ppb	85 °C, liq	2.4 min, rev	14
absorbance	50 ppb	ambient, liq	2.5 min, rev	12
absorbance	2−20 ppm	ambient, liq	1 min, rev	13
absorbance	85 ppb	ambient, liq	2−4 min	9
fluorescence	170 ppb	ambient, liq	2−5 min, rev	11
reflectance	25−1000 ppm	ambient, air	20 s	10
Au/WO_3	5ppb-50 ppm	450 °C, air	20 s, rev	2
$Zn_xGeO_yN_z$	100−200 ppm	100−300 °C, air	3 min, rev	5
$Cr_{1.8}Ti_{0.2}O_3$	100 ppm	300−550 °C	15 min, rev	6
AgCl	144−14400 ppb	100−170 °C	5 min, rev	7
polymer/Cu	0−10000 ppm	ambient, air	1 min, rev	8
BAW	0.5−20 ppm	ambient, air	20 s, rev	16

based on transition metal phosphonates[18] offer an interesting alternative to layered chalcogenides, because the size and chemical affinity of the binding pocket for ammonia and other analytes can be engineered in a rational manner. The synthesis, structure, and intercalation behavior of divalent metal phosphonates, $M^{II}(O_3PR)\cdot H_2O$ (M = Mg, Ca, Mn, Fe, Co, Ni, Cu, Zn, Cd; R = alkyl, aryl), have been studied by several research groups.[19−21] These compounds can be easily prepared from aqueous solution via precipitation or reduction. Some of them can be dehydrated topochemically to leave open M^{II} coordination sites, the size and shape of which are determined by the nature of the R group. These coordinatively unsaturated metal ions then act as shape-selective Lewis acid sites, which bind (reversibly or irreversibly, depending on the metal) Lewis bases of appropriate dimensions.

We previously reported a sensor that exploits the highly shape-selective binding of ammonia to dehydrated zinc phenylphosphonate.[22] Despite the selectivity of the intercalation reaction, the high surface area of the colloidal films used in that study caused substantial interferences from other Lewis base analytes. In this paper, we describe a modification of this strategy that minimizes both interferences and solid-state diffusion effects. The sensing element, copper biphenylbis(phosphonate), is a layered solid that is designed at the molecular level to allow ammonia to bind reversibly, once irreversible binding sites are saturated, while excluding chemically similar but larger analytes. The problems of nonspecific surface sorption and slow solid-state diffusion are simultaneously minimized by assembling the solid as a smooth, ultrathin (<70 Å) film on the electrodes of a thickness-shear mode resonator, more commonly called a quartz crystal microbalance (QCM) device, which detects the intercalation reaction as a mass (frequency) change. While ammonia diffusion in and out of these self-assembled films is slow, considering their extreme thinness, the device response time is still within the range of most conventional ammonia sensors.

EXPERIMENTAL SECTION

Reagents and Synthetic Procedures. High-purity ammonia and argon were obtained from Matheson Gas Co. (East Rutherford, N. J.). All other chemicals used were analytical grade and were obtained from Aldrich Chemical Co., Inc. (Milwaukee, WI).

Synthesis of 4,4′-Biphenylbis(phosphonic acid). The 4,4′-biphenylbis(phosphonic acid) used for film growth was synthesized from a photocatalyzed reaction of the brominated starting material with triethyl phosphite under illumination by a medium-pressure 450-W Hg lamp for 30 h.[23] Upon completion of the reaction, the mixture was washed once with water and the excess triethyl phosphite was removed by vacuum distillation, leaving the product (4,4′-biphenylphosphonate tetraethyl ester) as a white residue. This was hydrolyzed with a relux of ethanol−hydrochloric acid (5:7 v/v) for 6 h. The liquid was evaporated to give the 4,4′-biphenylbis(phosphonic acid), which was filtered and further purified by recrystallization from absolute ethanol. The structure of the product was verified by proton NMR.

Preparation of $Cu_2(O_3PC_6H_4-)_2$. Typically 100 mL of a 0.01 M (95% ethanol) solution of the bis(phosphonic acid) was mixed quickly with 50 mL of a 0.025 M aqueous solution of $Cu(NO_3)_2\cdot 2H_2O$, precipitating the salt as a green powder. This was suction filtered, washed several times with distilled water and ethanol, air-dried, crushed, and then dried in an oven at 100 °C for several hours. Ammonia-intercalated samples were obtained by exposure of the green solids to ammonia vapor in a closed system for several hours.

Growth of Thin Films of $Cu_2(O_3PC_6H_4-)_2$ on Gold Surfaces. *Layer Growth.* Planar substrates for ellipsometry and grazing-angle FT-IR studies and the gold electrodes of the QCM devices were carefully cleaned with Piranha solution (30% H_2O_2−concentrated H_2SO_4 1:4). Following the application of a 4-mercaptobutylphosphonic acid (MBPA) anchoring layer, sequential dipping into solutions of first the metal and then the alkyl- or arylbis(phosphonic acid) produces multilayer structures (See Scheme 1). Typically, QCMs and gold-on-glass subtrates were

(18) Aoki, K.; Brousseau, L. C., III; Mallouk, T. E. *Sens. Actuators B* **1993**, *14*, 703.

(19) (a) Cao, G.; Lee, H.; Lynch, V. M.; Mallouk, T. E. *Inorg. Chem.* **1988**, *27*, 2781. (b) Cao, G.; Lynch, V. M.; Swinnea, S. J.; Mallouk, T. E. *Inorg. Chem.* **1990**, *29*, 2112. (c) Cao, G.; Mallouk, T. E. *Inorg. Chem.* **1991**, *30*, 1434.

(20) (a) Zhang, Y.-P.; Cleafield, A. *Inorg. Chem.* **1992**, *31*, 2821. (b) Wang, R.-C.; Zhang, Y.-P.; Hu, H.; Frausto, R. R.; Clearfield, A. *Chem. Mater.* **1992**, *4*, 864. (c) Frink, K. J.; Wang, R.-C.; Colon, J. L.; Clearfield, A. *Inorg. Chem.* **1991**, *30*, 1438. (d) Zhang, Y.-P.; Scott, K. J.; Clearfield, A. *Chem. Mater.* **1993**, *5*, 495; Zhang, Y.-P.; Scott, K. J.; Clearfield, A. *J. Mater. Chem.* **1995**, *5*, 315.

(21) (a) Bujoli, B.; Palvadeau, P.; Rouxel, J. *Chem. Mater.* **1990**, 2, 582. (b) Bujoli, B.; Pena, O.; Palvadeau, P.; LeBideau, J.; Payen, C.; Rouxel, J. *Chem. Mater.* **1993**, *5*, 582.

(22) Brousseau, L. C., III; Aoki, K.; Garcia, M. E.; Cao, G.; Mallouk, T. E. *Multifunctional Mesoporous Inorganic Solids*; Sequeira, C., Hudson, M. J., Eds.; NATO ASI Series C 400; Kluwer: Boston, MA, 1993; pp 225−236.

(23) (a) Plumb, J. B.; Obrycki, R.; Griffin, C. E. *J. Org. Chem.* **1966**, *31*, 2455. (b) Obrycki, R.; Griffin, C. E. *J. Org. Chem.* **1968**, *33*, 632.

Scheme 1. Idealized Drawing of Layer-by-Layer Growth of a Copper Biphenylbis(phosphonate) Thin Film on a Gold QCM Electrode, and Reversible Intercalation of Ammonia

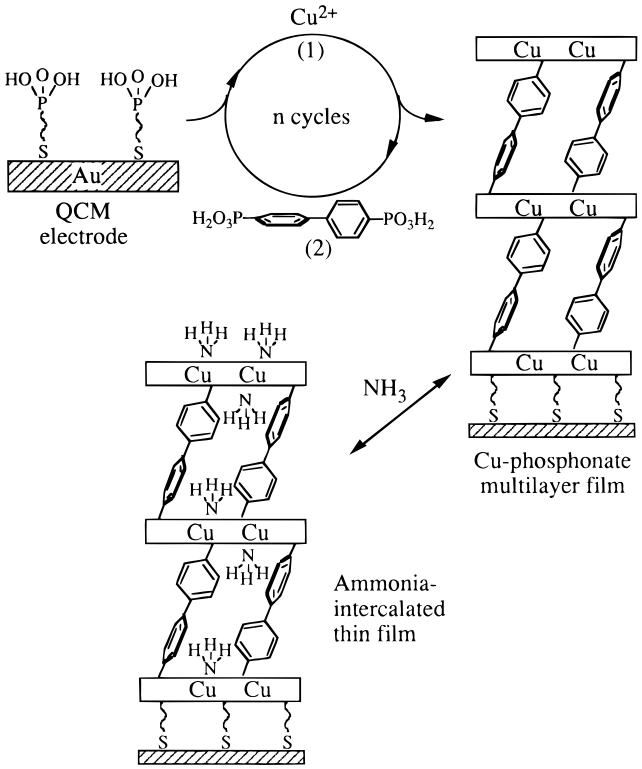

soaked overnight in a 2−3 mM solution of the anchoring agent, washed successively with water and ethanol (95%), and blown dry with argon. The samples were then alternately immersed in 3−5 mM ethanolic (95%) solutions of $M(NO_3)_2$ (M = Zn or Cu) and biphenylbis(phosphonic acid) for 30 min. Careful washing with water and ethanol (95%) after each step removes unbound reagents and prevents the formation of microcrystals of the metal phosphonate salt, ensuring monolayer growth with each adsorption step. Solutions were replenished after five adsorption cycles. After the desired number of films had been grown, the samples were blown dry with an argon stream and placed in an oven at 100 °C for 1−2 h to remove any adsorbed water or ethanol.

Ellipsometry and Infrared Spectroscopy. Ellipsometric measurements of film thickness were made with a Rudolf 437 ellipsometer. Glass slides were prepared with 1000 Å of evaporated Au (99.999%) (Evaporated Metal Films Corp., Ithaca, NY) deposited on a 50-Å Cr adhesion layer. Film thickness was calculated using the gold refractive index, $\eta_s = (1.119 \pm 0.002) - (1.750 \pm 0.100)i$, determined from a blank sample with $\lambda = 632.8$ nm. Optical constants for Au were in agreement with literature values. For the anchoring layer the refractive index was assumed to have $\eta_f = 1.540 - 0.000i$, giving $\Psi = 43.75$ and $\Delta = 108.72$, and a calculated thickness of ~7 Å. This value was used as a baseline for the metal phosphonate layers. The refractive index of $Cu_2(O_3PC_6H_4-)_2$ films, $\eta_f = 1.59 - 0.00i$ was estimated by the immersion method as follows: a small amount of the powdered solid was placed in each of seven small vials containing 2 mL of benzene, bromoform, benzyl alcohol, aniline, bromobenzene, xylidine, and carbon disulfide. None of these solvents dissolve $Cu_2(O_3PC_6H_4-)_2$. Suspensions in which the solid and liquid could barely be distinguished were found only with bromoform ($\eta_d = 1.595$) and aniline ($\eta_d = 1.584$), giving an estimate of the real part of the refractive index to an accuracy of ~±0.01. The imaginary part was assumed to be zero.

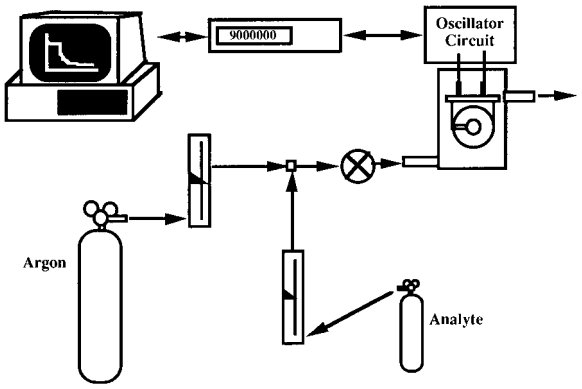

Figure 1. Experimental setup for QCM experiments, showing oscillator circuit, counter, computer, and series of manometers for control of gas flow and mixing.

The structural composition of the powders and films was confirmed by FT-IR. The powders were examined using the KBr pellet method and the films using grazing angle reflection−absorption on gold substrates. FT-IR spectra were recorded on a Nicolet 730 FT-IR at 4 cm^{-1} resolution for the powders and at 2 cm^{-1} for thin films. An acceptable signal-to-noise ratio was attained by averaging 1024 scans for the film samples. Because of the small absorbances of the thin films, 20−30 min purging with dry nitrogen to remove water and carbon dioxide from the background is essential, as is the careful preparation of a freshly cleaned gold reference sample. Reference samples were cleaned in Piranha solution as described above, rinsed with water and absolute ethanol, blown dry with an Ar stream, and placed immediately into the nitrogen-purged optical bench of the FT-IR.

Preparation of Sensing Devices, Instrumentation, and Experimental Design. Quartz crystal microbalances were prepared by the sequential adsorption method described above, with 5 and 20 layers of copper biphenylbis(phosphonate). The adsorption sequence was terminated by addition of a Cu layer.

Experiments were carried out using AT-cut quartz crystals with gold electrodes and a resonant frequency of 9 MHz (International Crystal Manufacturing Co., Inc., Oklahoma City, OK). A home-built oscillator circuit was used to drive the quartz crystal at its resonant frequency, with a 5-V dc power supply. The frequency of the QCMs was measured with a Philips PM 6654C programmable high-resolution counter (Fluke Technical Center, Rockville, MD) connected to a microcomputer which recorded the data. The circuit, power supply, and sample cell were insulated from external electromagnetic fields by placing them into a copper mesh Faraday cage, which was well grounded. The entire system is sketched schematically in Figure 1.

The use of QCMs as sensors is well documented and reviewed elsewhere.[24,25] These devices consist of a thin quartz wafer sandwiched between two electrodes. An oscillating current is applied, causing a shear oscillation of the crystal. Mass changes (Δm) on either electrode result in a dampening of the frequency

(24) (a) Bruckenstein, S.; Swathirajan, S. *Electrochim. Acta* **1985**, *30*, 851. (b) Buttry, D. A. In *Electroanalytical Chemistry;* Bard, A. J., Ed.; Marcel Dekker: New York, 1990; Vol. 17, p 1. (c) Ward, M. D.; Buttry, D. A. *Science* **1990**, *249*, 1000. (d) Buttry, D. A.; Ward, M. D. *Chem. Rev.* **1992**, *92*, 1355.

(Δf) of these oscillations, which are related by the Sauerbrey equation,[26]

$$\Delta f = \frac{-2\Delta m f_o^2}{A\sqrt{\rho_q \mu_q}} \quad (1)$$

in which μ_q and ρ_q are the shear modulus and density of quartz (respectively, 2.95×10^{11} dyn/cm^3 and 2.65 g/cm^3), A is the electrode area, and f_o is the resonant frequency. With the devices used in this work, which oscillate at 9-MHz device and have an electrode area of 0.21 cm^2, a 1-Hz change in the resonant frequency corresponds to a mass change of 1.15 ng on one of the electrodes.

A glass sample cell was fabricated with leads for the QCM that allowed flowing gas mixtures to be passed over both electrode surfaces. The initial resonance frequency for the QCM in each experiment was determined under a background of flowing argon gas. Gas mixtures were prepared by combining a partial pressure of analyte gas with the argon stream using calibrated manometers. For very low gas concentrations, double dilution of the ammonia stream was accomplished with a two-stage manometer arraingement. In the case of liquid analytes such as water and butylamines, a vapor pressure was generated by bubbling an argon stream through a volume of the liquid kept at a constant temperature by a chilled water bath. The vapor pressure was then calculated from the Clausius−Clapeyron equation and used to calculate the percent concentration (v/v) of the analyte gas. The ΔH_{vap} values were obtained from tabulated data.[27]

RESULTS AND DISCUSSION

Growth and Characterization of $Cu_2(O_3PC_6H_4-)_2$ Multilayer Films. Metal phosphonate films can be grown in layer-by-layer fashion on surfaces by sequential adsorption of the appropriate metal ions and alkyl- or arylbis(phosphonic acids).[28,29] Scheme 1 illustrates the film growth process and the binding of ammonia to coordinatively unsaturated Cu^{II} sites in the film.

The film growth process was monitored by mass changes, detected by QCM, by infrared spectroscopy, and by ellipsometry. A plot of the QCM frequency change vs layer number is shown in Figure 2. The QCM electrodes have a surface roughness factor (srf) of 2.0 ± 0.2, as determined electrochemically in a previous study.[29] Using a surface area of 25.4 Å^2/molecule[29] for the anchoring layer (MBPA), and a surface area of 0.422 cm^2 (total for both electrodes), the number of moles of anchoring agent on the crystal should be 2.8×10^{-10} for monolayer coverage on a smooth surface of gold. This would correspond to a frequency shift of −21 Hz, or −41 Hz for srf = 2. The actual change was found to be −51 Hz, indicating a srf of ~2.5. Based upon a similar calculation of the average molecular area (27.2 Å^2, using the unit cell data above), a smooth layer of Cu-terminated $Cu_2(O_3PC_6H_4-)_2$ should contain 2.6×10^{-10} mol, giving a frequency change of −49 Hz (or 98 Hz for srf = 2.0). From Figure 2, the frequency change is linear with layer number ($R = 0.9987$), and the slope gives a change per layer of −111 Hz, corresponding to the deposition of 5.8×10^{-10} mol $Cu_2(O_3PC_6H_4-)_2$ per layer, The five-layer device had a frequency change of −559 Hz, corresponding to 1.3×10^{-6} g of $Cu_2(O_3PC_6H_4-)_2$ on the electrodes, or 2.9×10^{-9} mol (theoretical, 2.6×10^{-9} mol for srf = 2.0). A plot of layer thickness, measured by ellipsometry, vs layer number (Figure 2), gives average layer spacings of 13.7 Å ($R = 0.9903$), consistent with QCM data, and in good agreement with the layer repeat distance determined by X-ray diffraction (see below), 13.97 Å.

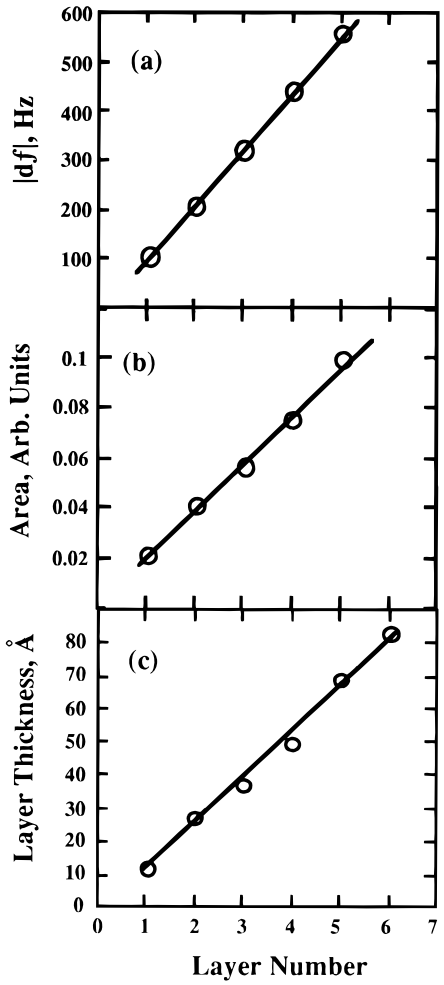

Figure 2. Layer plots for growth of $Cu_2(O_3PC_6H_4-)_2$ thin films on gold: (a) frequency change vs layer number; (b) peak area vs layer number for the 1148-cm^{-1} infrared absorbance band; (c) ellipsometric layer thickness vs layer number.

Grazing-angle FT-IR spectra of the $Cu_2(O_3PC_6H_4-)_2$ multilayer films are shown in Figure 3. Adsorption of a thin film on a conductive surface enhances those modes with a large component of dipole change normal to the plane of the substrate.[30] For this reason, the C═C (1439.6 cm^{-1}) and P−O stretching frequencies (1000−1150 cm^{-1}) dominate the thin-film spectrum. Similarly, the

(25) (a) Grate, J. W.; Patash, S. J.; Abraham, M. H. *Anal. Chem.* **1995**, *67*, 2162. (b) Tsionsky, V.; Gileadi, E. *Langmuir* **1994**, *10*, 2830. (c) Yan, Y.; Bein, T. *J. Phys. Chem.* **1992**, *96*, 9387. (d) Grate, J. W.; Wenzel, S. W.; White, R. M. *Anal. Chem.* **1991**, *63*, 1552. (e) Grate, J. W.; Klusty, M. *Anal. Chem.* **1991**, *63*, 1719.

(26) (a) Sauerbrey, G. *Z. Phyz.* **1959**, *155*, 206. (b) Sauerbrey, G. *Z. Phys.* **1964**, *178*, 457.

(27) Stull, D. *The Chemical Thermodynamics of Organic Compounds*; J. Wiley & Sons: New York, 1957.

(28) (a) Lee, H.; Kepley, L. J.; Hong, H.-G.; Mallouk, T. E. *J. Am. Chem. Soc.* **1988**, *110*, 618. (b) Lee, H.; Kepley, L. J.; Hong, H.-G.; Akhter, S.; Mallouk, T. E. *J. Phys. Chem.* **1988**, *92*, 2597. (c) Cao, G.; Hong, H.-G.; Mallouk, T. E. *Acc. Chem. Res.* **1992**, *25*, 420.

(29) Yang, H.; Aoki, K.; Hong, H.-G.; Sackett, D. D.; Arendt, M. F.; Yan, S.-L.; Bell, C. M.; Mallouk, T. E. *J. Am. Chem. Soc.* **1993**, *115*, 11855.

(30) Porter, M. D.; Bright, T. B.; Allara, D. L.; Chidsey, C. E. D. *J. Am. Chem. Soc.* **1987**, *109*, 3559.

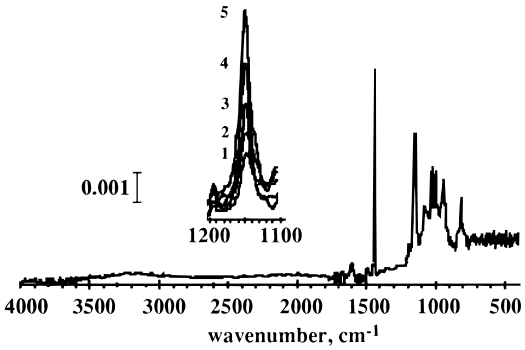

Figure 3. Reflection−absorption FT-IR spectra of a five-layer thin film of $Cu_2(O_3PC_6H_4-)_2$ on gold. Inset shows the absorbance in the P−O stretching region for one to five-layer films.

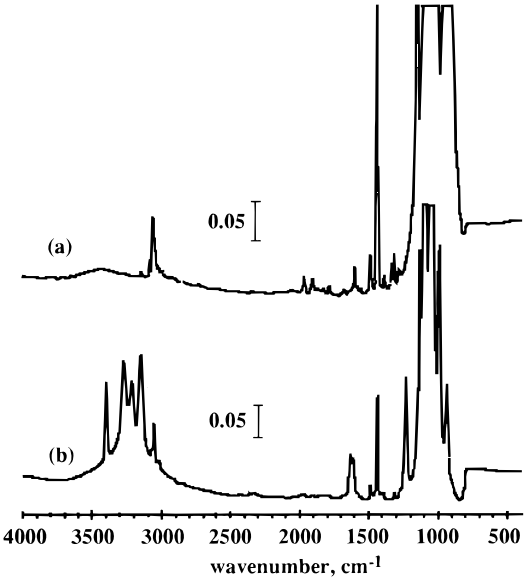

Figure 4. (a) FT-IR absorption spectrum of $Cu_2(O_3PC_6H_4-)_2$ pellet (in KBr); (b) spectrum of $Cu_2(O_3PC_6H_4-)_2 \cdot n NH_3$ ($2 < n < 4$).

C−H stretching frequencies are greatly attenuated in the film in comparison to the bulk sample (Figure 4), but the aromatic C−H wagging absorptions (816 cm^{-1}) are much stronger in the film, because of the orientation of C−H bonds relative to the surface plane. In solid $Cu(O_3PC_6H_5)\cdot H_2O$, the phenyl rings are tilted ~78° from the metal layer plane.[31] It might be expected that the biphenyl analogue will be make a similar angle to the plane, orienting the C═C bonds roughly perpendicular to it. The aromatic C−H bonds should lie within 30° of the plane, and their stretching modes should thus have a larger component in the plane than along the surface normal. The linearity of the film growth ($R = 0.9959$) is again confirmed by the growth in the peak height for the asymmetric (PO_3) stretch at 1148 cm^{-1}, shown as an inset in Figure 3.

Taken together, the QCM, ellipsometry, and FT-IR results indicate that well-ordered and oriented thin films, which resemble the bulk solid structurally, are deposited by the sequential adsorption method.

Structural Characterization and Intercalation Reactions of $Cu_2(O_3PC_6H_4-)_2$. X-ray powder diffraction patterns of the microcrystalline solid were indexed to an orthorhombic cell with $a = 7.573(2)$, $b = 7.436(2)$, and $c = 13.972(9)$ Å in good agreement with predicted values based on the phenylphosphonate salt.[20a] The powders were not highly crystalline, however, and the detailed crystal structure could not be obtained from X-ray powder data. Clearfield and co-workers have reported the same phase in their study of copper biphenylbis(phosphonate) salts,[32] with similar difficulty in the refinement of the structure. They reported a layer spacing of 14.0 Å, corresponding to a structure cross-linked by bis(phosphonates). Their TGA and FT-IR studies also indicate the absence of lattice water or phosphonate protons in the structure, meaning that the copper is coordinated by a distorted trigonal bipyramid of phosphonate oxygens. A similar coordination environment was found for anhydrous $Cu(O_3PC_2H_5)$.[33]

Table 2. Infrared Spectra

assignment	bulk (cm^{-1})	film (cm^{-1})
H_2O (background)	1606	3530−3920
		1604
		1430−1850
C═C str (aromatic)	1440	1440
C−H str (aromatic)	3056	
C−H bend (aromatic)	939	942
C−H wag (aromatic)	825	816
ν_{as} (PO_3)	1148	1149
		1081
ν_s (PO_3)	1061	1027
	1034	1013
	1019	999

Intercalation of ammonia changed the solid from a pale green to a deep blue, and this color faded over time upon standing in air. Samples of the unintercalated solid and the deeper blue and the faded blue solids were sent for C, H, N analysis in order to determine their composition. The green sample returned values of 32.70% C and 2.8% H (theory, 32.96% C and 1.84% H) confirming its formulation as anhydrous $Cu_2(O_3PC_6H_4-)_2$. The dark blue solid gave 28.39% C, 4.86% H, and 9.74% N, corresponding to approximately two intercalated molecules of NH_3 per Cu^{2+} (theory, 28.52% C, 3.99% H, and 11.09% N). The paler blue solid gave 30.20% C, 3.67% H, and 5.39% N, indicating one molecule of ammonia per Cu^{2+} (theory, 30.58% C, 2.99% H, and 5.94% N) in the final solid. The hydrogen content for all of the samples is slightly higher than expected, perhaps from water in the samples. Although there is no coordinated water in the structure, the metals and phosphonate head groups are polar, and a substoichiometric amount of water could bind at defect sites in the solid.

FT-IR spectra of $Cu_2(O_3PC_6H_4-)_2$ are shown in Figure 4a, and the spectrum of the ammonia-intercalated solid is shown in Figure 4b. Assignments are listed in Table 2.[34] Both spectra are dominated by C−H bending and asymmetric PO_3 stretching vibrations in the 800−950 cm^{-1} region, so the plots are expanded along the absorbance scale to give a better view of the aromatic ν(CH) at 3055.6 cm^{-1} and ν(C═C) at 1440.0 cm^{-1} absorption bands. The intercalated samples were prepared from bulk powder kept under gaseous ammonia in a small vial for several hours. The lower plot clearly shows the addition of ammonia, as

(31) Zhang, Y.; Clearfield, A. *Inorg. Chem.* **1992**, *31*, 2821.

(32) Poojary, D. M.; Zhang, B.; Bellinghausen, P.; Clearfield, A. *Inorg. Chem.* **1996**, *35*, 4942.

(33) Bideau, J. L.; Bujoli, B.; Jouanneaux, A.; Payen, C.; Palvadeau, P.; Rouxel, J. *Inorg. Chem.* **1993**, *32*, 4617.

(34) (a) Nakanishi, K.; Solomon, P. H. *Infrared Absorption Spectroscopy*; Holden-Day, Inc.: San Fransisco, 1977. (b) Nakamoto, K. *Infrared and Raman Spectra of Inorganic and Coordination Compounds*; J. Wiley & Sons: New York, 1986.

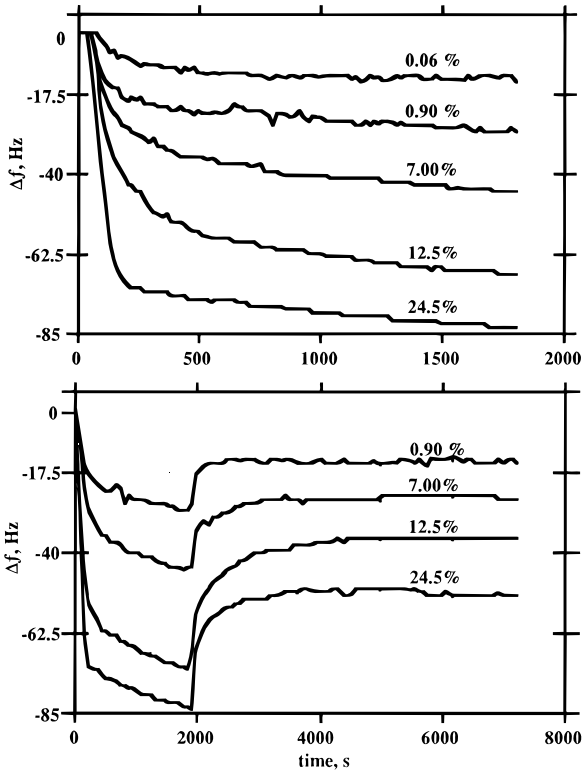

Figure 5. Δf vs time for intercalation of NH_3 into five layers of $Cu_2(O_3PC_6H_4-)_2$ on a QCM. Ammonia concentrations (v/v in Ar): 0.06, 0.90, 7.00, 12.5, and 25.4%. Upper trace shows intercalation, and lower trace shows intercalation and Ar purge on a longer time scale.

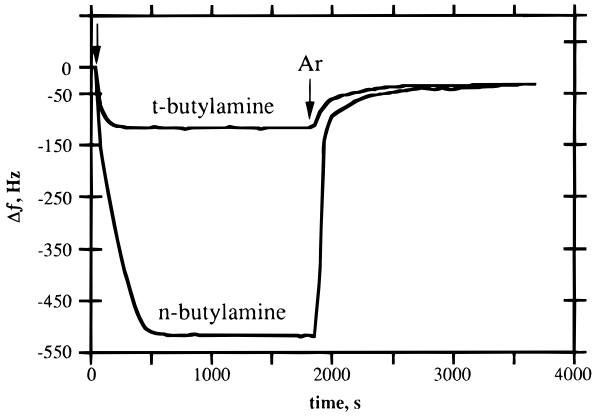

Figure 6. Δf vs time for exposure of a 20-layer $Cu_2(O_3PC_6H_4-)_2$ film to 4% (v:v) *tert*- and *n*-butylamine in Ar. Analyte injection and Ar purge are indicated by arrows.

evidenced by N−H stretching modes in the 3150−3400-cm^{-1} range, and asymmetric and symmetric bending vibrations at 1626.7 and 1608.9, and 1236.7 cm^{-1}, respectively.

Sensing of Ammonia in Copper Biphenylbis(phosphonate) Thin Films on a Quartz Crystal Microbalance. The QCM devices prepared with copper biphenylbis(phosphonate) films were exposed to a series of gas mixtures containing ammonia in Ar. Concentrations ranged from 0.01 to 47.4% (v/v), as generated by the manometer configuration described above. As with thin films grown by deposition of colloidal metal phosphonates,[22] the initial response in quite rapid as outer sites are filled and the reaction becomes limited by diffusion into the inner layers. The five-layer films become saturated at the higher concentrations (above 20%). Figure 5 shows frequency vs time curves for several concentrations spanning the useful range of the device. By reversing the intercalation reaction with a purge gas, it is evident that some of the ammonia is irreversibly bound, and after 90 min under flowing argon ∼64% remains in the film. As expected from diffusion models (vide infra), the desorption of ammonia from the film proceeds at a slower rate than its sorption. The saturation limit calculated from the sorption curves is 1.88×10^{-7} g of NH_3, compared with 1.84×10^{-7} g calculated from the amount of $Cu_2(O_3PC_6H_4-)_2$ deposited on the electrodes of the device. Hence all the sorbed ammonia can be accounted for, within experimental error, by intercalation rather than by physisorption at film defect sites.

The response of a 20-layer device to *tert*-butylamine and *n*-butylamine is shown in Figure 6. The changes in frequency are −116 and −517 Hz, corresponding to 3.66×10^{-9} and 1.63×10^{-8} mol, respectively. On a molar basis, both of these values are less than the response of the 20-layer device with the lowest concentration of ammonia used (0.01%), 2.03×10^{-8} mol. The device returns to the same residual value (∼−30 Hz) in each case under argon purge. This behavior quite is different from that of ammonia, where a substantial fraction of the bound analyte adsorbs irreversibly. Comparing the residual amount of butylamine (9.61×10^{-10} mol) with the theoretical amount per layer (roughly 3.0×10^{-9} mol) suggests that the two butylamines irreversibly saturate only one-third of the sites available in the outer layer. The very limited response of the device to these size-excluded amines contrasts markedly with the behavior of rough QCM sensor films prepared by the colloidal self-assembly and phosphonating techniques described previously.[22] The bulkier *tert*-butyl isomer in particular is substantially excluded from sorption sites within the copper bis(phosphonate) film. This shape selectivity is consistent with previous studies of amine intercalation in divalent transition metal phosphonates.[19−21]

Calculation of Partition and Diffusion Coefficients of Ammonia in Copper Biphenylbis(phosphonate) Thin Films. For gas-phase molecules diffusing into ultrathin films or membranes on a QCM, the frequency vs time data can be used to calculate the diffusion coefficient and partition constants for various sorption sites using the "time-lag" technique, which was originally developed for the analysis of diffusion into glassy polymers.[35−37] This approach is derived from the treatment of diffusion of a gaseous species into a glassy polymer film where it interacts by means of one of two modes: solution into the matrix or sorption into microcavities within the film. This model assumes that the sorption process involving the microvoids is irreversible and that diffusion into the interior of the film is due to transport through the matrix. There is a Henry's law partition function associated with the solubility of the gas in the polymer and a Langmuirian adsorption constant associated with the microcavities. The total amount (mass) of analyte sorbed by the film is therefore

(35) Vieth, Wolf R. *Diffusion In and Through Polymers: Principles and Applications*; Oxford University Press: New York, 1991.
(36) Bard, A. J.; Faulkner, L. R. *Electrochemical Methods: Fundamentals and Applications*; Wiley: New York, 1980; Derivation and discussion from Chapters 4 and 5 and Appendix A.
(37) (a) Kesting, R. E.; Fritzsche, A. K. *Polymeric Gas Separation Membranes*; Wiley: New York, 1993. (b) Frisch, H. L. *J. Phys. Chem.* **1957**, *61*, 93.

represented by

$$M(p) = M_i(p) + M_r(p) = k_i p + M_{r\infty} bp/(1 + bp) \quad (2)$$

where $M_{r\infty}$ is the (mass) saturation limit for the irreversible sites, for a partial pressure, p, of analyte in the ambient. A plot of M vs p will be concave, with a linear portion at low pressures where the sorption behavior is primarily irreversible, and a linear high-pressure section of primarily reversible, Langmuirian behavior, connected by a nonlinear "bend". (The presentation given here differs from the original in that the concentrations of species in the films are represented as mass changes, and $M_j = \Delta M_j$.) In the case of the copper phosphonate films, these sites correspond to the two sites of binding on the copper atoms, one of which is reversible and the other that is irreversible, designated S_r and S_i, respectively. This is the ideal case of the "dual-mode transport" model, since the two sites are evenly dispersed throughout the film and one is completely irreversible.

The two sorption processes in the copper bis(phosphonate) film can be separated by exposing the film to a high concentration of ammonia initially, in order to completely fill the irreversible sites. Subsequent sorption will therefore only occur at reversible sites and allow calculation of the association constant for these sites. A plot of p/M_r vs p is linear with a slope of $1/M_{r\infty}$ and am intercept of $1/bM_{r\infty}$. This result can then be introduced into the original expression and provide calculation of M_i by subtracting the reversible component at each pressure.

$$M_i(p) = M(p) - M_r(p) = kp \quad (3)$$

A plot or M_i vs p will be linear through the origin and have a slope of k.

The dual sorption/dual transport model accommodates calculation of the diffusion coefficients for the two modes by use of the "time-lag technique". According to this model, the amount of diffusant passing through the film, or the *permeation flux*, Q, is a function of the diffusion coefficient of the species and the concentration gradient in the film,

$$Q = -D\left(\frac{\partial M}{\partial l}\right) = -D\left(\frac{M_o - M_1}{\mathrm{d}l}\right) \quad (4)$$

where M_o and M_1 and the amounts of diffusant at the ambient/film interface and the electrode/film interface, respectively. If it is assumed that M_1 is zero (valid at short times of the process), this simplifies to an equation in M_o only. A related term is the *permeability*, P, defined by eq 5. This equation demonstrates the

$$P = -Ql/\Delta p = Dk \quad (5)$$

origins of permeability in Henrian sorption process (e.g., the sorption of organic vapors into rubber films) and, therefore, its relationship to the applied partial pressure of diffusant. Note that in the low-concentration limit, both the Henrian and Langmuirian isotherms are linear with analyte concentration, so the choice of isotherm for the low-pressure, irreversible part of the isotherm is arbitrary. By solving Fick's laws under the appropriate boundary conditions, it can be shown that the time-dependent form of the permeation flux, Q_t, is approximated by

$$Q_t = \frac{DM_o}{l}\left(t - \frac{l^2}{6D}\right) = \frac{DM_o}{l}(t - \Theta) \quad (6)$$

where D is the apparent diffusion coefficient and Θ is defined as the "time lag." An expression can also be derived for the permeability in terms of the diffusion coefficients of the two separate modes, given by eq 7, where $F = (D_r/D_i)$ and $K = (M_{r\infty}b/$

$$P = \frac{D_i M_r}{p_o}\left(1 + \frac{FK}{1 + bp}\right) = kD_i\left(1 + \frac{FK}{1 + bp}\right) \quad (7)$$

k). A plot of P vs $1/(1 + bp)$ is linear with slope of $bD_rM_{r\infty}$ and intercept kD_i, providing the individual diffusion coefficients. The effective diffusion coefficient, D_{eff}, is simply the sum of the coefficients for the two different processes.

To be useful in determining the diffusion coefficients in the copper phosphonate films this treatment must be related to experimental observables, in this case the mass change monitored by the QCM. Consider first that a plot of Q vs t will be linear with a slope, given by eq 8, that is directly proportional to the

$$\frac{\partial Q}{\partial t} = \frac{DM}{l} = \frac{Pp}{l} \quad (8)$$

permeability and can be directly related to the mass change in the film. This is evident by comparing the units of P (g·cm^2/s·Torr) and Q (g·cm/s). A plot of M vs t has the same shape as the Q vs t curve (in units of g/s). Thus, we can write an expression for P in terms of dM/dt:

$$P = \left(\frac{Ql}{\Delta p}\right) = \left(\frac{\mathrm{d}M}{\mathrm{d}t}\right)\left(\frac{l^2}{p_o}\right) \quad (9)$$

This relation can be rationalized by thinking of the *permeation flux* as the time-dependent gradient of the diffusant within the film and the *permeability* as the pressure dependence of this function.

Diffusion of NH_3 into Films of $Cu_2(O_3PC_6H_4-)_2$ on a Quartz Crystal Microbalance. Using the dual-transport model described above, diffusion into the five-layer film was examined. In all cases the diffusion path length was taken to be 0.5 μm, based on a SEM studies of the QCM electrode surface, which show gold domains with an average lateral dimension of ~1 μm. Note that this macroscopic (relative to the film thickness) diffusion length assumes a highly anisotropic flow of reactants in and out of the film. The calculated diffusion coefficient is dependent upon the choice of the diffusion path length. If the film thickness (five layers 68 Å) is used, the fit of the data to the curves is unaltered, but the calculated diffusion coefficients are orders of magnitude smaller.

The model allows different diffusion rates for the two sites in the film and correlates well with the sorption processes involved. The first indication of this is in the plot of the mass change in the film vs partial pressure of ammonia. As predicted by the model, there are two linear portions to the curve, one at high and the other at low partial pressures. This can be seen in Figure 7, which also shows that the device becomes saturated at high partial pressures. In order to verify that the Langmuirian portion of the

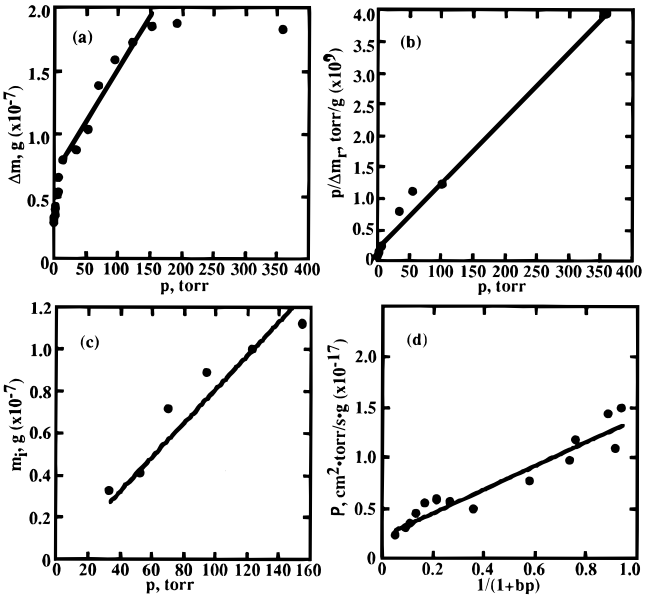

Figure 7. Sorption plots for the intercalation of NH_3 into five layers of $Cu_2(O_3PC_6H_4-)_2$ on a QCM: (a) Δm vs p, (b) p/m_r vs p, (c) m_i vs p, and (d) P vs $1/(1 + bp)$ for the intercalation of NH_3 into five layers of $Cu_2(O_3PC_6H_4-)_2$ on a QCM.

curve arises from reversible adsorption, the QCM was placed in a high concentration of ammonia for several hours, saturating the irreversible sites. The device was exposed to various ammonia concentrations until a stable resonance frequency had been reached and then purged with argon until the frequency returned to its original value. A typical response curve is shown in Figure 8. The intercalation is very rapid and is complete in less than 1 min. The removal of ammonia from the film takes longer, as expected. By comparison with data from unintercalated films, the amount of reversibly bound ammonia is the expected 50% of the total intercalated at each pressure.

The mass change/partial pressure data can be fit to a Langmuir adsorption isotherm as follows:

$$\theta = bp/(1 + bp) \tag{10}$$

$$1/\theta = 1/bp + 1 \tag{11}$$

where θ is the fractional coverage of ammonia, $m_r/m_{r\infty}$. Multiplying both sides of the equation by $p/m_{r\infty}$ we obtain eq 12, in which

$$p/m = 1/bm_{r\infty} + p/m_{r\infty} \tag{12}$$

the equilibrium constant b has units of $Torr^{-1}$. Reversible mass changes m_r are plotted in Figure 7b as p/m_r vs p. The slope of this plot gives a reversible saturation limit of 9.5×10^{-8} g, and the intercept divided by the slope returns an adsorption coefficient of 5.2×10^{-2} $Torr^{-1}$. From the meaured amount of $Cu_2(O_3PC_6H_4-)_2$ on the device, the saturation limit should be 9.4 $x10^{-8}$ g, in good agreement with the derived $m_{r\infty}$ value. The values for b and $m_{r\infty}$ were used to calculate the amount of ammonia bound at irreversible sites from the high pressure linear portion of Figure 7a, and a plot of m_i vs p is shown in Figure 7c. The slope of regression line is equal to the partition coefficient, $k_i = 8.1 \times 10^{-10}$ g/Torr.

Characterization of the irreversible and reversible ammonia sorption processes gives a measure of the sensitivity (defined as

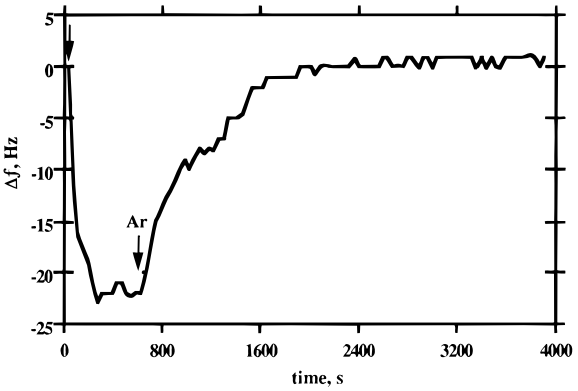

Figure 8. f vs time curve for ammonia intercalation into five layers of $Cu_2(O_3PC_6H_4-)_2 \cdot 2NH_3$ on a QCM.

the slope of the Δf vs % NH_3 curve) of these devices. Because this curve has two linear portions, the sensitivity is concentration-dependent. For reversible ammonia binding in a five-layer device in which the irreversible sites are already saturated, the slope is 2.9 Hz/% NH_3. In the lower concentration, irreversible region, the sensitivity is much greater, 44 Hz/% NH_3. The limit of detection (LOD) can be estimated as three times the root-mean-square deviation in the QCM response, which is $\sim\pm1$ Hz. This gives a LOD of $\sim$0.05% NH_3 in the irreversible regime. The useful range of the device therefore extends from 0.05 to $\sim$30% NH_3, where the reversible binding sites are substantially saturated at room temperature.

The *permeability*, P, is related to the slope of the $\Delta m/\Delta t$ curve at each partial pressure, according to eq 7, and when plotted against the quantity $(1/1 + bp)$ allows one to calculate the diffusion coefficients for the two sites. This plot is shown in Figure 7d. The slope of the regression line is 1.2×10^{-17}, giving a value for D_r of 2.3×10^{-9} ($\pm 8 \times 10^{-10}$) $cm^2 \cdot s^{-1}$. The intercept, 2.3×10^{-18}, gives a value of 3.3×10^{-9} ($\pm 8 \times 10^{-10}$) $cm^2 \cdot s^{-1}$ for D_i. The apparent diffusion coefficient, D_{eff}, is the sum of D_r and D_i, i.e., 5.6×10^{-9} ($\pm 8 \times 10^{-10}$) $cm^2 \cdot s^{-1}$. This value is comparable to typical diffusion coefficients of small molecules in polymers (10^{-10}–10^{-8} $cm^2 \cdot s^{-1}$) and zeolites (10^{-14}–10^{-9} $cm^2 \cdot s^{-1}$).[38] The comparison to zeolites is especially relevant, as gas transport through these media is slowed by reaction with the cavity walls.[37]

CONCLUSIONS

The copper salts of 4,4′-biphenylbis(phosphonic acid) are similar in structure and exhibit shape-selective intercalation reactions similar to that of copper phenylphosphonate. They can be made as bulk solids or as ultrathin films on gold surfaces. The solids and films show similar layer spacing and infrared spectra. Like the copper phenylphosphonates, the biphenylbis(phosphonates) can intercalate ammonia, which binds to the metal at two sites, one of which is reversible and the other irreversible at room temperature.

Derivatization of the gold electrodes of a quartz crystal microbalance with ultrathin films of copper biphenylbis(phosphonate) results in a device sensitive to low partial pressures of ammonia. The sensor detects the presence of the analyte in a flowing carrier gas via the coordination of NH_3 to copper atoms in the phosphonate lattice. The detection limit of the device

(38) Corma, A. In *Recent Advances in Zeolite Synthesis*; Klinowski, J., Barrie, P. J., Eds.; Elsevier: New York, 1989; Chapter 1.

depends on the number of layers of $Cu_2(O_3PC_6H_4-)_2$ grown on the surface, and a QCM device derivatized with 20 layers demonstrated a significant response at concentrations as low as 0.009% ammonia. The kinetic parameters for intercalation of the films can be calculated from the response curves, and an apparent diffusion coefficient of $\sim 5.6 \times 10^{-9}$ cm^2/s was obtained from the dual-transport model. The devices are regenerated between uses by heating to 100 °C, which removes the irreversible site-bound ammonia.

In comparison with the other sensing methods, the response time ($t_{90\%} \approx 9$ 0 s) of the devices described here is about average, although the response for the "doped" devices preintercalated with ammonia at the irreversible binding sites is faster. Amperometric and potentiometric sensors for ammonia require several minutes to reach equilibrium, as do most absorbance-based devices. Advantages are gained with devices based on copper bis(phosphonate) films in terms of sensing environment, since they monitor gas streams directly (i.e., they do not require acid−base indicator solutions or liquid electrochemical cells) and at ambient temperature. Fabrication of these devices is straightforward and provides control over the amount of sensing material and sensitivity.

Most importantly, this study demonstrates that it is possible to apply to a signal transduction device, as a self-assembled thin film, a solid-state material with a designed and crystallographically well-characterized binding site for a specific analyte. The accompanying paper[39] describes the rational modification of such binding sites, in order to adapt the sensor to a different analyte.

ACKNOWLEDGMENT

This work was supported by a grant from the National Science Foundation (CHE-9396243). Instrumentation for X-ray diffraction experiments was provided by NSF Grant DMR-9402860.

Received for review June 25, 1996. Accepted November 19, 1996.[⊗]

AC960630C

(39) Brousseau, L. C., III; Aurentz, D. J.; Benesi, A. J.; Mallouk, T. E. *Anal. Chem.* **1997**, *69*, 688.

[⊗] Abstract published in *Advance ACS Abstracts,* January 1, 1997.